

# Computationally Assessing Diamond as an Ultrafast Pulse Shaper for High Power Ultrawide Band Radar

Christopher C. Herrmann,<sup>1, a)</sup> Joseph Croman,<sup>2</sup> and Sergey V. Baryshev<sup>1, b)</sup>

<sup>1)</sup>Department of Electrical and Computer Engineering, Michigan State University, 428 S. Shaw Ln., East Lansing, MI 48824, USA<sup>c)</sup>

<sup>2)</sup>High Power Microwave Section, Code 5745, Naval Research Laboratory, 4555 Overlook Ave., SW Washington, DC 20375, USA

Diamond devices hold promise to reshape ultrafast and high power electronics. One such device is the diode avalanche shaper (DAS), which functions as an ultrafast closing switch where sub-nano-second closing is caused by the formation of the streamer traversing the diode much faster than  $10^7$  cm/s. One of the most prominent applications of DAS is in ultrawide band (UWB) radio/radar. Here we simulate a diamond-based DAS and compare the results to a silicon-based DAS. All DAS were simulated in 3D in mixed mode as ideal devices using the drift-diffusion model. The simulations show that diamond DAS promises to outperform Si DAS when sharpening kilovolt nanosecond input pulse.

## I. INTRODUCTION

Ultrawide band (UBW) radio/radar has become a promising area of radio frequency technology and continues to make inroads in communication, sensing and vision across consumer, commercial and military sectors. Its operating methodology is the same as traditional radar, but is unique in that UWB radar has a much wider frequency spectrum of transmitted pulses<sup>1</sup>. This permits sampling in both the frequency and time domains, a primary benefit of UWB. Another unique feature of UWB radio is its immunity to passive environmental interference as well as to interference in spatially and spectrum crowded conditions where multiple systems operate simultaneously. This makes it a critical technology for autonomous and connected systems. UWB radar performance, characterized by detection resolution and range, depends directly on both the duration and the power level of the pulse provided to the system. The shorter the pulse (the wider the band) the better the resolution. The higher the peak power the longer the range.

It is highly desired to have a solid state technology that can provide 10's of kilovolts in a single  $\lesssim 100$  ps pulse. Such technology could push the envelope of UWB radar capability. Other important disciplines could greatly benefit, including ultrafast electro-optics and laser technologies<sup>2</sup>, discharge/plasma-assisted combustion and chemistry<sup>3</sup>, bio-electro-magnetics<sup>4</sup>, and accelerator systems<sup>5</sup>.

Ultrashort pulses can be obtained using semiconductor step recovery diode (SRD) or Schottky diode<sup>6</sup>, but they can only commutate a few volts and have a low peak power. Si technology for opening (drift SRD, or DSRD)<sup>7</sup> and closing switches (diode avalanche shaper, DAS)<sup>8</sup> have been introduced. Both DSRD and DAS are

*p-i-n* diodes. When stacked, MW peak power low jitter pulses have been demonstrated with leading and trailing edges in the sub-ns range<sup>9</sup>. Some bipolar transistor circuits can be used but they work in the ns-range, and it takes 20 to 50 BJT's in the circuit<sup>10</sup> to match the voltage rating that a circuit with a few stacked diodes can produce.

Previous work on Si shapers<sup>11</sup> attempted to look beyond Si technology. Direct bandgap GaN and GaAs were ruled out for ultrafast high power applications due to the minority carrier lifetime being inherently short,  $\sim 10$  ns. No reasonable semiconductor offers both improved breakdown field and high mobility and lifetime except for diamond and SiC to potentially outperform Si. The team at Ioffe is actively exploring the potential of the SiC technology<sup>12-14</sup>. Presented here is an early attempt to assess the potential of diamond.

## II. OPERATING PRINCIPLE OF DAS

The pulse sharpening produced by the DAS is due to delayed ionization breakdown (in contrast to the common avalanche breakdown that takes place instantaneously) that forms a high charge plasma streamer travelling at a velocity much higher than the saturated drift velocity. The conventional transit time limitation is thus overcome. To form the streamer<sup>15</sup>, fast overvoltage (kilovolts on the nanosecond scale, reported as the voltage ramp rate  $dV/dt$ ) of a reversely biased diode must be provided (exemplary circuit arrangement is depicted in Fig. 1). With  $dV/dt \gtrsim 1$  V/ps, where the state-of-the-art Si DSRD technology can produce 2 V/ps<sup>7,16</sup>, avalanche breakdown does not instantaneously occur despite an applied voltage that can reach a few times higher than the dc breakdown voltage.

First, a displacement current  $j_d = \epsilon \epsilon_0 \partial E / \partial t$ , associated with time varying electric field, flows through the diode forming a pre-pulse voltage across the load (see Fig. 2). As electric field is established across the DAS, charges accelerate and produce electron-hole plasma in

<sup>a)</sup>Electronic mail: [herrmannc1899@gmail.com](mailto:herrmannc1899@gmail.com)

<sup>b)</sup>Electronic mail: [serbar@msu.edu](mailto:serbar@msu.edu)

<sup>c)</sup>On leave from Department of Electrical Engineering, University at Buffalo, Buffalo, NY 14260.

TABLE I: Comparison of Ultimate Material Properties

	Diamond	Si	4H-SiC
Bandgap $E_g$ (eV)	5.47	1.1	3.2
Breakdown field $E_{br}$ (MV/cm)	10	0.3	3
Electron Mobility $\mu_e$ (cm <sup>2</sup> /V·s)	4500	1450	900
Hole Mobility $\mu_h$ (cm <sup>2</sup> /V·s)	3800	480	480
Electron Saturation Velocity $v_s$ ( $\times 10^7$ cm/s)	2	0.86	3
Johnson's Figure of Merit $E_{br} \times v_s$ (V/ps)	200	2.6	90

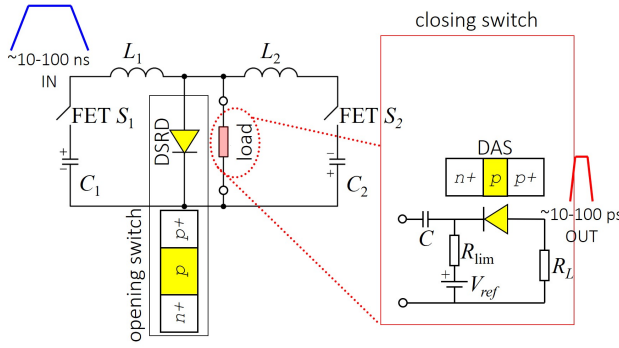


FIG. 1: A MMIC high power ultrafast circuit based on closing and opening switches, adapted from Refs.<sup>12</sup> and<sup>17</sup>. Simulated circuit is shown in red box.

the undoped/low doped, base (or, *i*-layer) of the device. This plasma continues to accumulate as  $n_p(t) = n_0 e^{v_s \alpha(E)t}$ , as long as the device does not break down. The rate of this plasma generation is directly related to the field dependent ionization coefficient  $\alpha(E)$  which is a material's property. When the plasma streamer forms, current flows freely and at plasma velocity  $v_p$  that is  $\sim 10$ -100 times higher than the saturated drift velocity  $v_s$ .  $v_p$  takes form<sup>14</sup>

$$v_p \sim v_s \frac{n_p}{n_d} \left( \frac{E_{max}}{E_{br}} - 1 \right) \frac{1}{\ln(\frac{n_p}{n_0})}, \quad (1)$$

here  $n_0$  ( $\gtrsim 10^9$  cm<sup>-3</sup>) is the initial background charge concentration in the depleted base,  $n_d$  ( $10^{14}$  cm<sup>-3</sup> in our case) is the doping concentration in the base layer,  $E_{max}$  is the maximum electric field of the overvoltaged *p-i-n* diode such that  $E_{max}/E_{br}$  is between 1 and 2.  $n_p$  is the plasma charge concentration that can be found as  $n_p \sim \frac{q \varepsilon \varepsilon_0 E_{br}}{q}$ , where  $q$  is the elementary charge,  $\varepsilon \varepsilon_0$  is a material permittivity. For diamond, it results in  $v_p \gtrsim 10^8$  cm/s. Streamers causing lightning are known to move as fast as  $\sim 10^7$ - $10^8$  cm/s<sup>18</sup>. Major factors that affect switching performance include thickness of the diode base layer  $L_i$ , breakdown voltage  $V_{br}$ , as well as the input voltage ramp rate  $dV/dt$ , a limitation that comes from the input pulse generator:

$$t_{lim1} = \frac{L_i}{v_p}, \quad (2)$$

$$t_{lim2} = \frac{V_{br} - V_{ref}}{dV/dt}, \quad (3)$$

where  $V_{ref}$  is a dc pre-bias. For  $L_i=10-100 \mu\text{m}$ , switching takes place on a sub-nanosecond time scale. Streamer enabled switching is the only non-optical method allowing for conductivity modulation of a semiconductor structure at 100 ps or faster.

### III. MODELLING METHODOLOGY

The main advantage of diamond over Si is two-fold. One is that a diamond DSRD paired with diamond DAS can produce voltage rates up to 200 V/ps (Table I) – it is easy to show that ultimate voltage rate is the Johnson's figure of merit. Second is that diamond  $\alpha(E)$  dependence is shifted to higher fields, resulting in faster multiplication and thus a thinner base in the *p-i-n* structure. Overall, this means that switching enabled by a diamond-based DAS can be much faster and DAS output voltage rate can be much higher than those produced by Si DAS. Evidence for this is seen from Fig. 2. The base *i*-layer is intentionally made ten/twenty-fold thinner than usually anticipated<sup>18,19</sup>, and results are compared to an optimized Si DAS design produced by work at the University of New Mexico by Focia *et al.*<sup>16</sup>. Replicating device doping and geometry studied by Focia *et al.* allowed for the cross-checking of our computational approach for Si DAS (Fig. 2a). From there, diamond was implemented as a custom material based on Watanabe's  $\alpha(E)$  data<sup>20</sup>. Early comparisons seen in Fig. 2b favors the 10  $\mu\text{m}$  diamond device over 75  $\mu\text{m}$  Si device<sup>19</sup>: peak output voltage rate (right axis) of diamond DAS is six times that of the Si DAS and diamond DAS exhibits a higher hold off voltage. Each dotted trace represents a transient voltage curve with the time derivatives of these curves being represented by the solid lines. The black curve shows the input pulse applied to the DAS while the colored curves represent devices simulated. Comparing results of Fig. 2a and b, it is clear that thinner base provides for better sharpening but at the cost of smaller output voltage: reducing the *i*-layer thickness of the Si DAS by 10 times improved switching from 259 to 37 ps but output voltage reduced from 2 to 0.5 kV. This is while diamond DAS with 10  $\mu\text{m}$  *i*-layer switched in 38 ps providing for 2.1 kV output voltage.

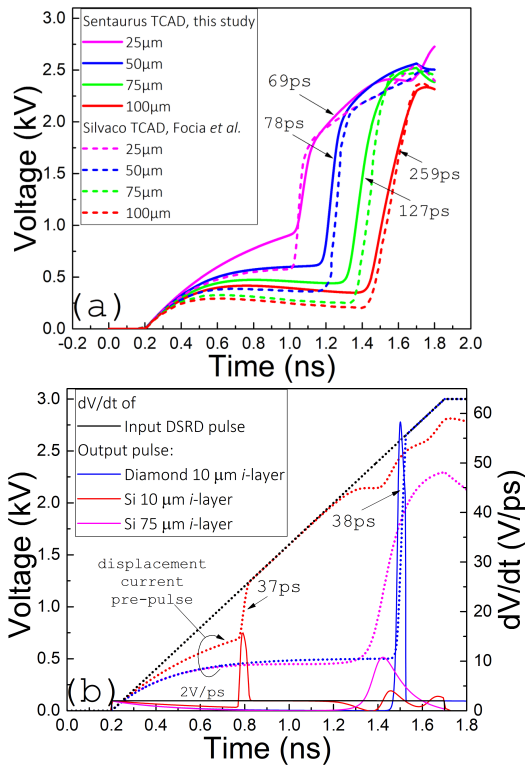


FIG. 2: Transient analysis of Si and diamond DAS: (a) benchmarking of the Sentaurus TCAD model to the previous results obtained for Si DAS<sup>16</sup>; (b) comparison between thin base, 10  $\mu\text{m}$ , Si and diamond DAS and thick base, 75  $\mu\text{m}$ , Si DAS. Arrows denote FWHM of the output voltage rate  $dV/dt$ .

The drift-diffusion approach was used to model the physical behavior of the DAS in three dimensions using the Synopsys Sentaurus TCAD software. This 3D model was configured to simulate constant carrier mobility, carrier velocity saturated at high fields, and avalanche dynamics in accord with the Van Overstraet de Man model<sup>21</sup>. Tunneling-assisted impact ionization was not simulated as it is expected to play no role for wide bandgap material based or minor role for canonical Si based DAS<sup>14</sup>. The DAS devices were simulated in the mixed mode which allowed for mixed physics and circuit SPICE-like transient analyses. The virtual circuit, shown in Fig. 1, consisted of a voltage source connected to the cathode of the diode with the anode connected to a  $50\ \Omega$  load resistor. The amplitude of the hypothetical DSRD based voltage source was ramped at a constant, linear rate, providing the input voltage with a rise rate of 1-100 V/ps for the DAS to sharpen. A dc voltage source and current limiting resistor were also applied to the cathode of the diode. This allows for the delayed ionization breakdown point to be tuned, see Eq. 3;  $V_{ref}$  was kept constant at 10 V.

#### IV. RESULTS AND DISCUSSION

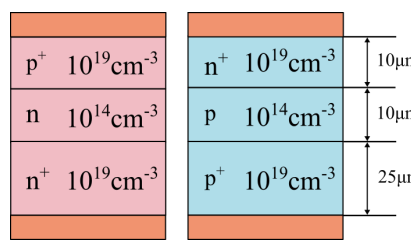


FIG. 3: Simulated silicon (pink) and diamond (blue) diode structure; doping and geometry are labeled.

To assess the advanced pulse sharpening capability enabled by diamond, the input ramp rates and the sharpened output voltage rates  $dV/dt$  are compared as a performance figure. There is of course no singular metric

that can ultimately capture the overall performance of a DAS as different applications require certain characteristics to be a priority. Nevertheless, a performance improvement between Si and diamond can be gleaned from Fig. 2. Comparison between 10  $\mu\text{m}$  and 75  $\mu\text{m}$  Si devices show no significant improvement in terms of peak output  $dV/dt$ . With all other parameters set the same, the thinner base Si DAS provides for faster switching, consistent with Eq. 2, but hold off voltage is reduced; and vice versa for the thicker base DAS. To further explore  $dV/dt$  performance, we chose to compare a 10  $\mu\text{m}$  base DAS made of Si and diamond, whose structures are shown in Fig. 3. The Si DAS has light *n*-doping in the base *i*-layer, like in the classical case<sup>8</sup>. The diamond DAS has light *p*-doping to reflect upon intentional or unintentional doping with boron that has lowest activation energy among all known dopants. Cross-sectional area of both DAS was 1  $\text{mm}^2$ .

The performance of the device is dependent on the slope  $dV/dt$  of the rising input voltage, the black line shown in Fig. 2b. The  $dV/dt$  of the pulse can be changed by holding pulse duration  $dt$  constant and varying ultimate voltage amplitude  $dV$ , or vice versa. These two methods are not equivalent, as shown by Fig. 4. When varying  $dt$ , the diamond DAS will begin to exhibit incomplete ionization and device performance will level off with ever shortening pulse duration that is necessary to achieve higher  $dV/dt$ . This incomplete ionization is thought to be due to the fact that crystal lattice, to be ionized, is unable to respond adequately to sub-ns pulses (phononic phenomena are on  $\sim\text{ns}$  time scale). The crystal lattice structure simply does not have enough time to react to the many-kV pulse applied to it.

Fig. 4 shows that for every given input voltage ramp rate increased through increasing  $dV$  at  $dt$  kept at 1.5 ns, diamond exhibited a higher output voltage rate. Ultimate input voltage ramp rates ranged from 1 to 100 V/ps, reflecting upon near future advances in diamond DSRD technology that could enable input pulses with such characteristics, see Johnson's figure of merit in Table I. Since single Si based DSRD can ultimately pro-

duce not more than 2 V/ps<sup>7</sup>, multiple Si DSRDs must be stacked together to overcome this 2 V/ps limitation. Recent review by Rukin<sup>5</sup> still cites the 80 kV 1.5 ns DSRD generator designed at Ioffe Institute<sup>22</sup> as the top of the line. From this, 50 V/ps is used as a cut-off input  $dV/dt$  that can be produced by the stacked Si technology.

On *log-log* scale, Fig. 4 demonstrates that for every given input voltage ramp rate the output voltage rate increased tenfold, providing an ultimate 1 kV/ps at the output when receiving an input of 0.1 kV/ps from a hypothetical ideal diamond DSRD. Given our simulation setting, such ultimate switching takes place on a 5 ps time scale (inset in Fig. 4) which would greatly expand the performance of a UWB radar. Such sharpening is enabled by operating the *p-i-n* structure with a thin base layer, which comes at the expense of the delivered peak voltage that dropped from 150 kV to 5 kV, still producing half a MW of peak power. As mentioned earlier, designing a DAS has to start with application requirements with primary consideration being given to the trade-off between high peak voltage and switching time, the trade-off clearly seen in Fig. 2a,b. Additional parameters of optimization also include varied doping levels and cross section area.

Since  $t_{lim1}$  is  $<<10$  ps for 10  $\mu\text{m}$  base DAS, it is instructional to compare computational results against Eq. 3. The inset in Fig. 4 shows that Eq. 3 overestimates the switching time (especially at lower input ramp rates) but correctly predicts the ultimate switching time. As in the simulation, simultaneous plasma generation and expansion across the *i*-layer is tracked through the  $\alpha(E)$  relation with no  $V_{br}$  set *per se*, one possible explanation of the observed discrepancy is that thinner base devices are more sensitive to the plasma self-consistent generation-expansion dynamics, as compared to canonical  $\gtrsim 100$   $\mu\text{m}$  base devices. The DAS structures presented in Fig. 3 are punched-trough diodes. Breakdown voltage utilized in Eq. 3 calculation were therefore deduced as  $V_{br} = V_{br}^{bulk} \left( \frac{L_i}{W_{SCR}} \right) \left( 2 - \frac{L_i}{W_{SCR}} \right)$ , where  $V_{br}^{bulk}$  is the breakdown voltage and  $W_{SCR}$  is the depletion region width for the one-sided abrupt junction<sup>23</sup>.

## V. CONCLUSION

It was shown computationally, that a DAS constructed from diamond exhibits superior performance when compared to identical diode structure made of Si: the output voltage rate was more than 3 times higher than that of the Si device which resulted in 10-fold increase in the output peak power for the same switching time. Special attention was paid to thin base devices to attest them for ultrafast high peak power pulse shapers in order to push the envelope in UWB radar applications. This demonstrates that 5-10 ps MW scale pulses are feasible with single crystal diamond homoepitaxy.

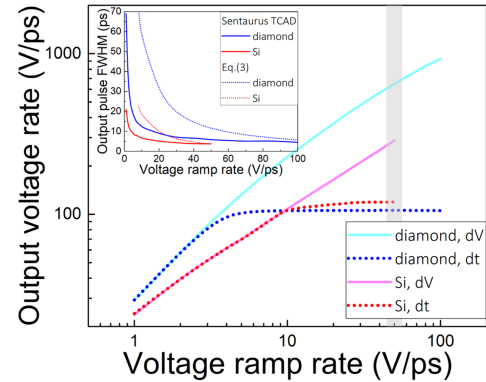


FIG. 4: Computed peak output voltage rate of DAS versus input voltage ramp rate from a hypothetical diamond DSRD producing up to 100 V/ps.

Performance difference of changing peak amplitude  $dV$  or pulse duration  $dt$  is emphasized. The inset compares resultant switching time (FWHM of the output voltage rate  $dV/dt$ ) as a function of input voltage ramp rate for Si and diamond DAS.

**Acknowledgments.** This work was sponsored by the Office of Naval Research under contract No.N6833520C0486. C.S.H. and S.V.B. were partially supported by funding from the College of Engineering, MSU, under Global Impact Initiative.

- <sup>1</sup>C. Nguyen and J. Han, *Time-Domain Ultra-Wideband Radar, Sensor and Components: Theory, Analysis and Design* (Springer, 2014).
- <sup>2</sup>M. R. Woolston, “Fast electronic driver for optical switches,” (Master thesis, Colorado State University, 2012).
- <sup>3</sup>S. M. Starikovskaia, “Plasma-assisted ignition and combustion: nanosecond discharges and development of kinetic mechanisms,” *Journal of Physics D: Applied Physics* **47**, 353001 (2014).
- <sup>4</sup>K. H. Schoenbach, S. J. Beebe, and E. S. Buescher, “Intracellular effect of ultrashort electrical pulses,” *Bioelectromagnetics* **22**, 440–448 (2001).
- <sup>5</sup>S. N. Rukin, “Pulsed power technology based on semiconductor opening switches: A review,” *Review of Scientific Instruments* **91**, 011501 (2020).
- <sup>6</sup>G. Wong Choi, J. Joo Choi, and S. Hoon Han, “Note: Picosecond impulse generator driven by cascaded step recovery diode pulse shaping circuit,” *Review of Scientific Instruments* **82**, 016106 (2011).
- <sup>7</sup>I. Grekhov, V. Efanov, A. Kardo-Sysoev, and S. Shenderey, “Power drift step recovery diodes (dsrd),” *Solid-State Electronics* **28**, 597 – 599 (1985).
- <sup>8</sup>I. V. Grekhov, A. F. Kardo-Sysoev, L. S. Kostina, and S. V. Shenderey, “High-power subnanosecond switch,” *Electronics Letters* **17**, 422–423 (1981).
- <sup>9</sup>L. M. Merensky, A. F. Kardo-Sysoev, A. N. Flerov, A. Pokryvailo, D. Shmilovitz, and A. S. Kesar, “A low-jitter 1.8-kV 100-ps rise-time 50-kHz repetition-rate pulsed-power generator,” *IEEE Transactions on Plasma Science* **37**, 1855–1862 (2009).
- <sup>10</sup>L. Jinyuan, S. Bing, and C. Zenghu, “High voltage fast ramp pulse generation using avalanche transistor,” *Review of Scientific Instruments* **69**, 3066–3067 (1998).
- <sup>11</sup>M. J. Chudobiak, *New Approaches For Designing High Voltage, High Current Silicon Step Recovery Diodes for Pulse Sharpening Applications*, Ph.D. thesis, Carleton University (1996).

<sup>12</sup>P. A. Ivanov and I. V. Grekhov, "High-voltage sharp-recovery 4h:sic drift diodes: Theoretical estimation of limiting parameters," *Technical Physics* **60**, 897–902 (2015).

<sup>13</sup>A. V. Afanasyev, B. V. Ivanov, V. A. Ilyin, A. A. Smirnov, A. F. Kardo-Sysoev, and S. A. Shevchenko, "A study of 4h-SiC diode avalanche shaper," *Journal of Physics: Conference Series* **917**, 082002 (2017).

<sup>14</sup>P. Rodin, P. Ivanov, and I. Grekhov, "Performance evaluation of picosecond high-voltage power switches based on propagation of superfast impact ionization fronts in sic structures," *Journal of Applied Physics* **99**, 044503 (2006).

<sup>15</sup>M. I. D'yakonov and V. Y. Kachorovskii, "Theory of streamer discharge in semiconductors," *Soviet Physics JETP* **67**, 1049 (1988).

<sup>16</sup>R. J. Focia, "Ultrafast high power switching diodes," (Master thesis, University of New Mexico, 1996).

<sup>17</sup>R. J. Focia, E. Schamiloglu, and C. B. Fleddermann, "Simple techniques for the generation of high peak power pulses with nanosecond and subnanosecond rise times," *Review of Scientific Instruments* **67**, 2626–2629 (1996).

<sup>18</sup>B. F. J. Schonland, "Progressive lightning. iv. the discharge mechanism," *Proceedings of the Royal Society of London. Series A, Mathematical and Physical Sciences* **164**, 132–150 (1938).

<sup>19</sup>R. J. Focia, E. Schamiloglu, C. B. Fleddermann, F. J. Agee, and J. Gaudet, "Silicon diodes in avalanche pulse-sharpening applications," *IEEE Transactions on Plasma Science* **25**, 138–144 (1997).

<sup>20</sup>T. Watanabe, M. Irie, T. Teraji, T. Ito, Y. Kamakura, and K. Taniguchi, "Impact excitation of carriers in diamond under extremely high electric fields," *Japanese Journal of Applied Physics* **40**, L715–L717 (2001).

<sup>21</sup>R. Van Overstraeten and H. De Man, "Measurement of the ionization rates in diffused silicon p-n junctions," *Solid-State Electronics* **13**, 583 – 608 (1970).

<sup>22</sup>V. Efanov, A. Kardo-Sysoev, M. Larionov, I. Tchashnikov, P. Yarin, and A. Kriklenko, "Powerful semiconductor 80 kv nanosecond pulser," in *Proc. 11th IEEE International Pulsed Power Conference* (IEEE, 1997).

<sup>23</sup>S. M. Sze and K. K. Ng, *Physics of Semiconductor Devices (3rd edition)* (Wiley, 2007).